Acta Pharmaceutica Sinica B 2019;9(1):186–193

Chinese Pharmaceutical Association
Institute of Materia Medica, Chinese Academy of Medical Sciences

Acta Pharmaceutica Sinica B

www.elsevier.com/locate/apsb
www.sciencedirect.com

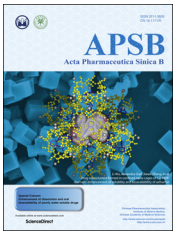

ORIGINAL ARTICLE

Interaction between human serum albumin and cholesterol-grafted polyglutamate as the potential carriers of protein drugs

Xiangxue Lyu[a], Qiufen Zhang[b], Dehai Liang[b,*], Yanbin Huang[a,*]

[a]*Key Laboratory of Advanced Materials (MOE), Department of Chemical Engineering, Tsinghua University, Beijing 100084, China*
[b]*College of Chemistry & Molecular Engineering, Peking University, Beijing 100871, China*

Received 10 March 2018; received in revised form 10 June 2018; accepted 11 June 2018

KEY WORDS

Protein drug delivery;
Polypeptide;
Self-assemble;
Human serum albumin;
Interaction;
Carrier

Abstract Currently there is no successful platform technology for the sustained release of protein drugs. It seems inevitable to specifically develop new materials for such purpose, and hence the understanding of protein–material interactions is highly desirable. In this study, we synthesized cholesterol-grafted polyglutamate (PGA-*g*-Chol) as a hydrophobically-modified polypeptide, and thoroughly characterized its interaction with a model protein (human serum albumin) in the aqueous solution by using circular dichroism, fluorescence methods, and light scattering. With the protein concentration fixed at 5 μmol/L, adding PGA-*g*-Chol polymers into the solution resulted in continuous blue shift of the protein fluorescence (from 339 to 332 nm), until the polymer molar concentration reached the same value as the protein. In contrast, the un-modified polyglutamate polymers apparently neither affected the protein microenvironment nor formed aggregates. Based on the experimental data, we proposed a physical picture for such protein–polymer systems, where the polymer first bind with the protein in a 1:1 molar ratio *via* a fraction of their hydrophobic pendant cholesterol resides along the polymer chain. In this protein/polymer complex, there are excess unbound cholesterol residues. As the polymer concentration increases, the polymers form multi-polymer aggregates around 200 nm in diameter *via* the same hydrophobic cholesterol residues. The protein/polymer complex also participate in the aggregation *via* their excess cholesterol residues, and consequently the proteins are encapsulated into the nanoparticles. The encapsulation was also found to increase the thermal stability of the model protein.

*Corresponding authors.
E-mail addresses: dliang@pku.edu.cn (Dehai Liang), yanbin@tsinghua.edu.cn (Yanbin Huang).

Peer review under responsibility of Institute of Materia Medica, Chinese Academy of Medical Sciences and Chinese Pharmaceutical Association.

https://doi.org/10.1016/j.apsb.2018.08.001

1. Introduction

Protein drugs have become an essential and fast-growing segment of modern medicine, and will be more and more important in the future[1]. In comparison with the small molecular drugs in terms of the pharmaceutical profile, proteins are too large and hydrophilic to be orally absorbed, and consequently their prevalent administration route is injection[2]. On the other hand, except for antibodies which have special recycling pathways *via* Fc receptors, many other proteins are not large enough to prevent their renal filtration and clearance[3]. In addition, proteins are susceptible to enzyme degradation, and these factors together result in protein drugs' short residence time in circulation. Frequent injection is often needed to maintain their therapeutically effective concentration[2–4]. As a typical example, interferon-α_{2b} (Intron® A), whose molecular weight is around 19 kDa, has an elimination half-life about 2 h and its serum concentration becomes undetectable just 4 h after intravenous infusion[5]. Therefore, it is desirable to develop sustained-release delivery systems for these protein drugs.

Initially, the biodegradable poly(lactic-*co*-glycolic acid) (PLGA) microsphere technology, which has been successfully used in more than a dozen small molecule and peptide drug products, was tried to encapsulate protein drugs to achieve sustained release[6]. However, unlike their small molecule or peptide counterparts, protein drugs are vulnerable to losing their native folded structure and proved to be generally incompatible with the PLGA microsphere technology, as evidenced by the withdrawal of the only protein-in-PLGA product (*i.e.* Nutropin Depot®) from the clinical use in 2004. Since then, little progress has been made in the protein/PLGA microsphere technology, and it seems that the introduction of new excipients is inevitable[7].

Among the new excipients being studied, the hydrophobically modified polypeptides attracted a great deal of attention. For example, vitamin E-grafted poly(glutamic acid) (Medusa®) was shown to self-assemble into nano-sized aggregates in water, which were stabilized by the hydrophobic association among the vitamin E moieties[8]. Interferon-α_{2b} was shown to spontaneously partition into these nanogels, and to be slowly released after injection and maintain a therapeutic concentration for about 6 days in human studies[8]. This polyglutamate-based material is biocompatible and biodegradable, and more importantly, the protein encapsulation process takes place spontaneously in the aqueous solution (*i.e.*, no organic solvent or detrimental interface was involved). Consequently, this type of polymers seems promising as a platform technology for protein sustained release, and it has proceeded to as far as Phase II clinical trials.[9] However, the interaction between proteins and the hydrophobically-modified polypeptides has not been studied in detail, and the physical picture of protein inside the nanogel is not clear yet, especially the interplay between protein–polymer interactions and polymer self-associations. Similarly, cholesterol-grafted pullulan has also been extensively studied as a protein delivery material[10,11], but its non-ionic polysaccharide backbone is significantly different from the charged polyglutamate chains. In addition, Lee et al.[12] synthesized poly(γ-glutamic acid)-cholesterol conjugates, and studied their aggregation profile and their effect on the refolding of denatured protein. Ma et al.[13] synthesized poly(ethylene glycol)-block-poly(γ-cholesterol-L-glutamate) and studied their properties as a carrier for hydrophobic, small molecular drugs.

In this study, we synthesized cholesterol-grafted poly(glutamic acid) (PGA-*g*-Chol) and studied in detail its interaction with a model protein, human serum albumin (HSA). Besides its easy availability, the other reason we chose HSA as the model protein is that it is the most abundant protein in the blood, and any intravenously-injected polymers will unavoidably interact with it, and hence the polymer-HSA interaction is also interesting beyond protein drug delivery.

2. Material and methods

2.1. Materials

Poly-L-glutamic acid sodium salt (α-PGA-Na) (molecular weight 15–50 kDa), oligo(ethylene glycol) 600 (OEG 600), pyrene and human serum albumin (recombinant, expressed in rice, lyophilized powder, HSA) were purchased from Sigma. Cholesterol, D-mannitol, adipoyl chloride, *N*-(3-dimethylaminopropyl)-*N*′-ethylcarbodiimide hydrochloride (EDC), 4-dimethylaminopyridine (DMAP), triethylamine, *N*,*N*-dimethylformamide (99.8%, super-dry) (DMF), benzophenone and all deuterated solvents were purchased from J&K Scientific (Shanghai, China). All other reagents were of analytical grade. All of the reagents except α-PGA-Na and toluene were used directly without further purification. Regenerated cellulose dialysis membrane (MWCO = 3500 Da) was purchased from YuanYe Bio-Technology (Shanghai, China).

α-Polyglutamic acid (α-PGA) was acidized by hydrochloric acid from α-PGA-Na and purified by centrifugation and lyophilization[14]. Toluene (150 mL) was dehydrated by Na (5.0 g) using benzophenone (0.5 g) as the indicator.

2.2. Synthesis and characterization of PGA-g-Chol

2.2.1. Synthesis of the oligo(ethylene glycol)-cholesterol conjugate (OEG-Chol)

The synthesis was done following the method from Proksch et al.[15] First, 1.16 g (0.003 mol) of cholesterol and 0.4 g (0.004 mol) of triethylamine were dissolved in 10 mL dry toluene as Solution A. Adipoyl chloride (0.76 g, 0.004 mol) was dissolved in 10 mL of dry toluene as Solution B. Solution A was slowly added (in 3 min) into solution B in ice-water bath and the mixture was stirred for 1.5 h. Then, the mixture was filtered to remove the triethylamine hydrochloride precipitate and obtain Solution C. 3.6 g (0.006 mol) of OEG 600 and 0.6 g (0.006 mol) of triethylamine were dissolved in 10 mL of dry toluene as Solution D. Solution C was added (in 3 min) into solution D in ice-water bath. After 1.5 h, triethylamine hydrochloride was filtered off and the reaction mixture was extracted four times with 15 mL of 21% (*w*/*w*) NaCl solution. Toluene was removed from the organic phase by rotary evaporation, and 15 mL of methanol was added to the remaining light-brown, waxy material and the insoluble matter was removed by filtration. Then, methanol was removed by rotary evaporation to obtain OEG-Chol as the product, which was characterized by ^{1}H NMR (Supporting Information Fig. S1, $CDCl_3$, 300 MHz, JNM-ECA300 Spectrometer).

2.2.2. Synthesis of PGA-g-Chol

50.0 mg of α-PGA (0.4 mmol glutamic acid monomer units), 16.0 mg (0.02 mmol, 5% (mol/mol) of the glutamic acid units) of OEG-Chol, 7.5 mg of EDC (0.04 mmol) and 2.4 mg of DMAP (0.02 mmol) were added into 2 mL of dry DMF. The mixture was stirred at room temperature for 48 h. The product PGA-*g*-Chol-5 (whose feeding ratio of OEG-Chol and glutamic acid units was 5%, mol/mol) was purified by dialysis against deionized water

(regenerated cellulose membrane, MWCO 3500 Da) and followed by lyophilization. PGA-*g*-Chol-10 was synthesized similarly with the OEG-Chol amount doubled.

2.2.3. Characterization of PGA-g-Chol

The chemical structure of PGA-*g*-Chol was characterized by ^{1}H NMR, ^{13}C NMR and DOSY NMR. PGA-*g*-Chol (10 mg) was dissolved in 550 μL of D_2O (pD was adjusted to 7.0 ± 0.1) and the grafting degree of OEG-Chol was determined from the integral intensity ratio of the methylene peaks of α-PGA to the OEG group peaks of OEG-Chol. In addition, the NMR spectrum of PGA-*g*-Chol in DMF-d_7 was used to detect the hydrophobic cholesterol moieties. DOSY-NMR was used to detect whether the polymer systems contained any small molecule residues, and the characterization was carried out on the same NMR spectrometer as in other NMR analysis.

2.3. Characterization of PGA-g-Chol aggregation with and without HSA

2.3.1. Sample preparation

All PGA-*g*-Chol samples except those used for TEM characterizations were prepared in 10 mmol/L PBS (pH = 7.0 ± 0.1, containing 5% (*w*/*w*) mannitol). Mannitol was added to make the solution isotonic and hence better simulating an injectable solution. For TEM characterization, the polymer samples did not contain mannitol to avoid the complication of mannitol crystals formed after solvent evaporation. For samples containing human serum albumin (HSA), the concentration of HSA was chosen to be 5 μmol/L to minimize the self-aggregation of the proteins. The mixtures solution was stored at 4 °C overnight to ensure homogeneous mixing.

2.3.2. Critical aggregation concentration determination

The critical aggregation concentration (CAC) was determined for PGA-*g*-Chol by the pyrene fluorescence method[16]. An aliquot (100 μL) of pyrene solution (2×10^{-5} mol/L in ethanol) was added to a glass vial and evaporated in vacuum to form pyrene thin film. 1.0 mL PGA-*g*-Chol solution was added to the glass vial and the resulting mixture was stirred in a TS-100C shaking incubator (TENSUC, 25 °C, 230 rpm) for 24 h. The final concentration of pyrene in the mixture was 2×10^{-6} mol/L. The fluorescence emission spectra were recorded using a Hitachi F-7000 fluorescence spectrophotometer equipped with a thermo-regulate' cell compartment with $\lambda_{exc} = 319$ nm; the ratio between the fluorescence intensity at $\lambda_{em} = 373$ nm (I_1) and at $\lambda_{em} = 384$ nm (I_3) was calculated for each sample and results were plotted as a function of PGA-*g*-Chol concentration. The CAC value was taken as the break point of the I_3/I_1–PGA-*g*-Chol concentration curve.

2.3.3. Dynamic and static light scattering (DLS and SLS) characterizations

The aggregate size of PGA-*g*-Chol in solution was measured by DLS and SLS on a BI-200SM Goniometer (Holtsville, NY, USA). The illuminant was a He-Ne laser (633 nm, 17 mW, vertical polarization, Newport, CA, USA). The sample solution was directly filtered (0.45 μm, Sartorius Stedim Biotech, Goettingen) into the measuring cell. SLS measurements were carried out over the angular range from 30° to 90° at room temperature. The polymer concentrations were varied from 0.25 to 2.5 mg/mL.

In SLS measurements, the mean square radius of gyration (R_g) can be calculated by the following Eq. (1):

$$HC/R_{VV}(\theta) = (1/MW)\,[1 + (1/3)\,R_g^2 q^2] + 2A_2C \quad (1)$$

where optical constant $H = 4\pi^2 n^2 \left(dn/dc\right)^2 / \left(N_A \lambda^4\right)$, C is the solution concentration, $q = 4\pi n/\lambda \sin\left(\theta/2\right)$, n, dn/dc, and λ respectively represent Avogadro constant, the increment of solvent and solute reflection indexes, and optical wavelength. A_2 is the second Virial coefficient, $R_{VV}(\theta) = R_{VV,t} n^2 (I_s - I_0)/\left(I_t n_t^2\right)$, where I_s, I_0, and I_t are respectively the light intensity of solution, solvent and toluene; n and n_t are respectively reflection index of solvent and toluene; $R_{VV,t}$ is the Rayleigh scattering factor of toluene. When the optical wavelength is 633 nm, $R_{VV,t} = 1.4 \times 10^{-5}\,cm^{-1}$.

In DLS measurements, the line width distribution and diffusion coefficient can be obtained and further converted into the hydrodynamic radius (R_h) by using the Stokes-Einstein equation:

$$D = (k_B T)/(6\pi\eta R_h) \quad (2)$$

where k_B, T, η are the Boltzmann constant, the absolute temperature, and the viscosity of the solvent, respectively.

2.3.4. Transmission electron microscopic (TEM) observation

One mL of PGA-*g*-Chol (0.1 mg/mL) was mixed with 20 μL of tungstophosphoric acid aqueous solution (2.0%, *w*/*w*). After 1 h, 30 μL of the mixture was dropped on a carbon-coated 300 mesh copper grid and dried in vacuum. TEM observation was carried out on a Hitachi H-7650B (80 kV, 25 °C).

2.4. Interaction between PGA-g-Chol and HSA

2.4.1. Circular dichroism (CD) spectrum

CD spectra were recorded on a Chirascan circular dichroism spectrometer (Applied Photophysics) at a 1.0 nm interval from 260 to 200 nm. Experiments were performed in a rectangular cell with optical path of 0.1 cm. The concentrations of α-PGA and PGA-*g*-Chol were 1.0 mg/mL. In the experiment to study thermal stability of HSA, all samples were treated at 90 °C for 1 h, cooled down, and then stayed at room temperature for another hour before measurement.

2.4.2. Protein fluorescence measurements

The fluorescence emission spectra were recorded using a Hitachi F-7000 fluorescence spectrophotometer equipped with a thermo-regulated cell compartment with $\lambda_{exc} = 295$ nm. In the meantime, the fluorescence intensity at 593 nm, which is basically the scattered light at 90°, was used to qualitatively characterize the aggregation of PGA-*g*-Chol.

3. Results and discussion

3.1. Characterization of PGA-g-Chol

Initially, we tried to directly graft the cholesterol units onto the α-PGA main chain *via* esterification. However, the solubility of cholesterol in DMF turned out to be too low for the reaction. Instead, we first conjugated an oligo(ethylene glycol) (OEG) linker to the cholesterol units, and the resulted OEG-Chol was found suitable for the following conjugation to the α-PGA main chain (Scheme 1).

The grafting degree of PGA-*g*-Chol was varied by changing the amount of OEG-Chol used in the reactions, and experimentally

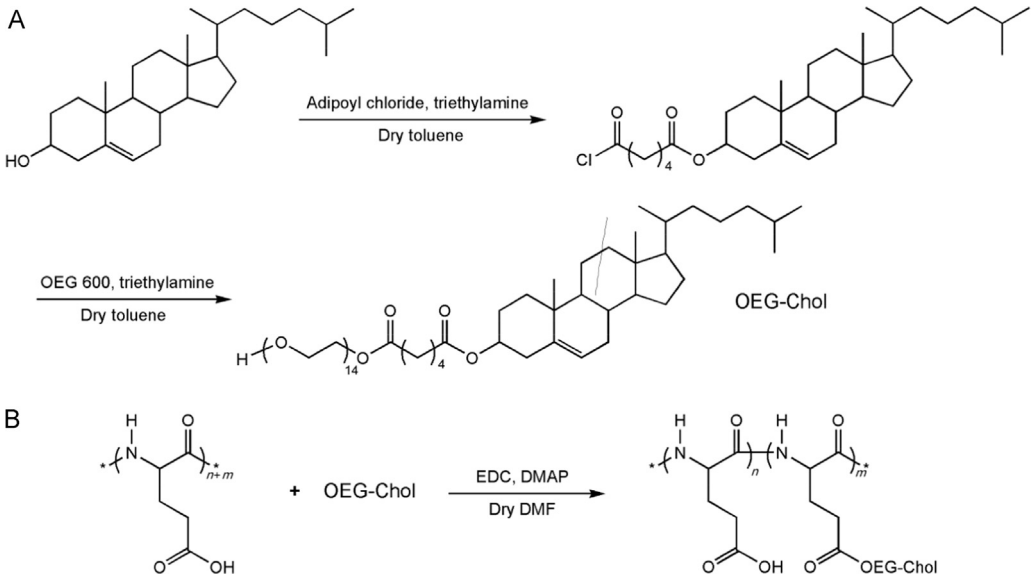

Scheme 1 Synthesis schemes of (A) OEG-Chol and (B) PGA-*g*-Chol.

Table 1 Characterization of PGA-*g*-Chol in the PBS solution (pH 7.0±0.1, 10 mmol/L PBS, with 5% (*w*/*w*) mannitol).

Sample	Feeding ratio[a]	Grafting degree[b]	Aggregate diameter[c] (nm)	CAC[d] (mg/mL)
PGA-*g*-Chol-5	0.050	0.032	~150	0.06
PGA-*g*-Chol-10	0.100	0.065	~200	0.02

[a]Feeding ratio stands for the molar ratio of OEG-Chol and glutamic acid units in the reaction.
[b]The grafting degree stands for the molar ratio of OEG-Chol and glutamic acid units of PGA-*g*-Chol experimentally determined by ^{1}H NMR.
[c]The particle diameter was measured in PBS by DLS.
[d]CAC was measured by the pyrene fluorescence method.

determined by NMR (Supporting Information Figs. S2–S4 and Table 1). For the product PGA-*g*-Chol-5, about one out of every 30 glutamate units was conjugated, while the grafting degree was doubled for PGA-*g*-Chol-10. Since the molecular weight of the initial α-PGA-Na polymers was 15–50 kDa, there were 3–10 and 6–20 cholesterol moieties on each polymer chain of PGA-*g*-Chol-5 and PGA-*g*-Chol-10, respectively. Diffusion NMR (in D_2O) was used to test whether the product contained ungrafted OEG-Chol (Supporting Information Figs. S5–S8). The diffusion coefficient of the α-PGA polymer was about 3.86×10^{-11} m^2/s (Supporting Information Fig. S5), while that of OEG-Chol was one order of magnitudes higher (about 1.30×10^{-10} m^2/s, Supporting Information Fig. S6). In contrast, the diffusion NMR spectrogram of PGA-*g*-Chol shows only one band at the same order of magnitudes with α-PGA (about 2.80×10^{-11} m^2/s for PGA-*g*-Chol-5 and 2.64×10^{-11} m^2/s for PGA-*g*-Chol-10, Supporting Information Figs. S7 and S8), suggesting that the conjugated polymers were free from small molecular impurities.

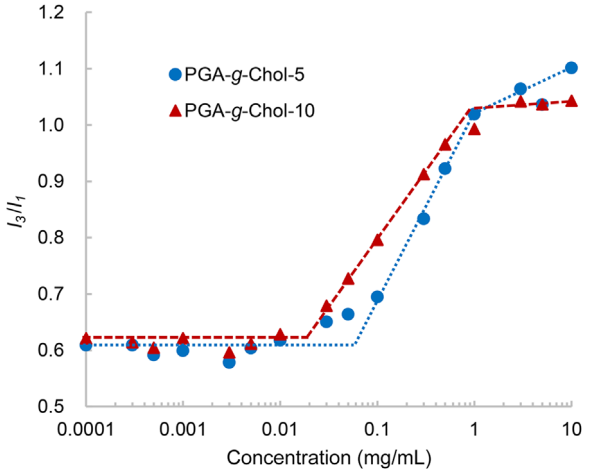

Figure 1 Intensity ratio I_3/I_1 obtained from the fluorescence excitation spectra of pyrene plotted versus the PGA-*g*-Chol-5 and PGA-*g*-Chol-10 concentrations (0.0001–10 mg/mL).

3.2. *Self-aggregation of PGA-g-Chol in water*

We first determined the CACs of the two polymers in the aqueous solution by the pyrene fluorescence method (Fig. 1). The I_3/I_1 values remains unchanged over the low PGA-*g*-Chol concentration range until a certain point (*i.e.*, CAC) and then increases sharply with the polymer concentration, indicating that hydrophobic domains were formed in the aqueous solution and pyrene was partitioned in them. As indicated by the trend lines in Fig. 1, PGA-*g*-Chol-5 and PGA-*g*-Chol-10 in aqueous solution showed CAC values around 0.06 and 0.02 mg/mL, respectively.

We then characterized the aggregates formed by PGA-*g*-Chol at concentrations higher than their CACs (Supporting Information Figs. S9 and S10). Fig. 2 shows their aggregate sizes (the

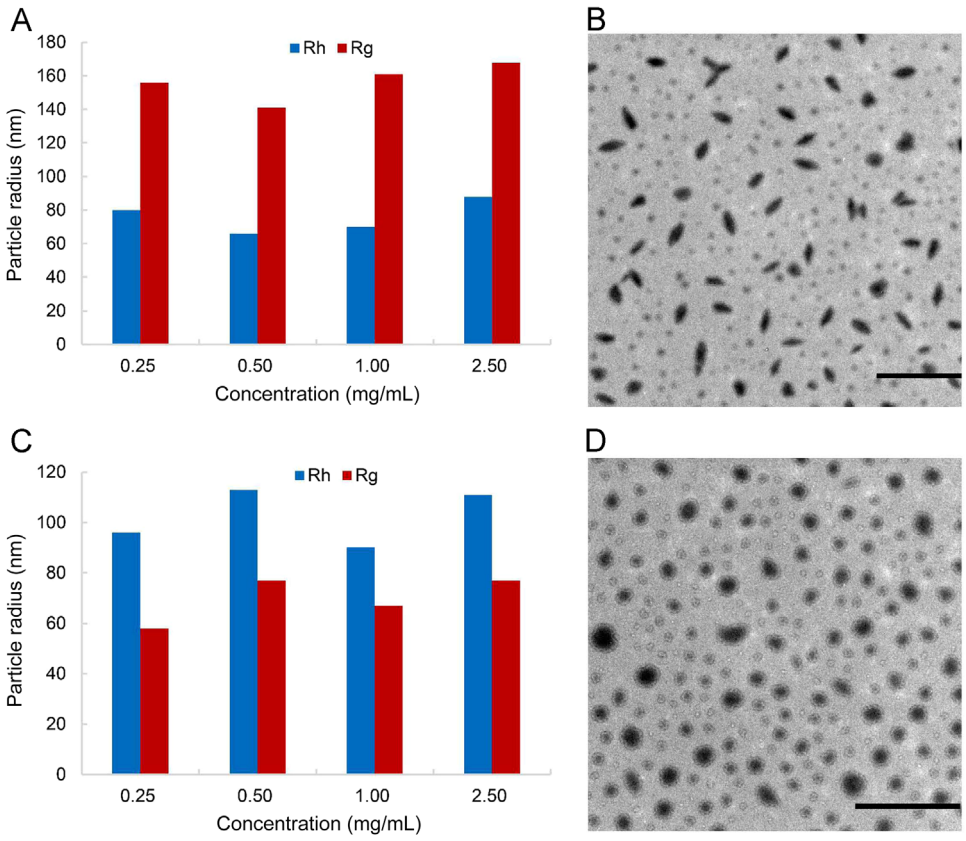

Figure 2 Aggregate particle sizes as determined by DLS and SLS for (A) PGA-*g*-Chol-5 and (C) PGA-*g*-Chol-10 at different concentrations. TEM images of (B) PGA-*g*-Chol-5 and (D) PGA-*g*-Chol-10 aggregates (both at 0.1 mg/mL). TEM samples were stained with phosphotungstic acid. Scale bars represent 1 μm in both TEM images.

hydrodynamic radius R_h and the radius of gyration R_g) determined by DLS, SLS and TEM. For both polymers, the sizes of aggregates did not change much over the polymer concentration range of 0.25 to 2.5 mg/mL. The aggregate R_h values were around 75 and 100 nm for PGA-*g*-Chol-5 and PGA-*g*-Chol-10, respectively. In contrast, the aggregate R_g values were 150 and 70 nm for PGA-*g*-Chol-5 and PGA-*g*-Chol-10, respectively. It is interesting that shapes of PGA-*g*-Chol-5 and PGA-*g*-Chol-10 aggregates seemed to be different, as evidenced by their significantly different R_g/R_h ratios. For PGA-*g*-Chol-10, the R_g/R_h ratio was 0.7, suggesting the aggregates were close to hard spheres[17]. In contrast, the R_g/R_h ratio of PGA-*g*-Chol-5 aggregates was about 2, corresponding to ellipsoid shapes[17]. We indeed observed ellipsoid-shaped aggregates in the PGA-*g*-Chol-5 samples coexisting with sphere-shapes aggregates in the same TEM image. Currently, it is unclear to us why PGA-*g*-Chol-5 formed ellipsoidal aggregates. However, the other aspects of the aggregation profiles of PGA-*g*-Chol-5 and PGA-*g*-Chol-10 seemed similar enough, so only PGA-*g*-Chol-10 system is presented in the following sections (results of PGA-*g*-Chol-5 systems are included in the Supporting Information as Figs. S11–S13).

3.3. *Interaction between PGA-g-Chol and HSA*

As mentioned before, we are particularly interested in the interplay between the PGA-*g*-Chol self-aggregation and its interaction with proteins. To begin with, we studied the effect of polymers on the conformation of HSA using circular dichroism. Since polyglutamates also contribute to the CD signals, the spectra of HSA in the presence of PGA-*g*-Chol or *α*-PGA were obtained by deducting the pure PGA-*g*-Chol or *α*-PGA spectrum (at the same concentrations) from those of the HSA/PGA-*g*-Chol (or *α*-PGA) mixture system. The helix-rich secondary structures of HSA largely remained in the presence of both PGA-*g*-Chol and *α*-

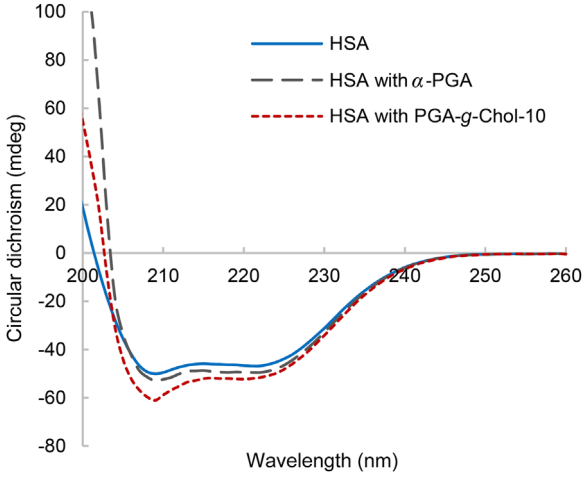

Figure 3 CD spectra of HSA in different solutions. The spectrum of HSA (5 μmol/L) with PGA-*g*-Chol-10 (1.0 mg/mL) (or *α*-PGA, 1.0 mg/mL) was obtained by subtracting PGA-*g*-Chol (or *α*-PGA) spectrum from those of HSA/PGA-*g*-Chol (or *α*-PGA) mixture solutions.

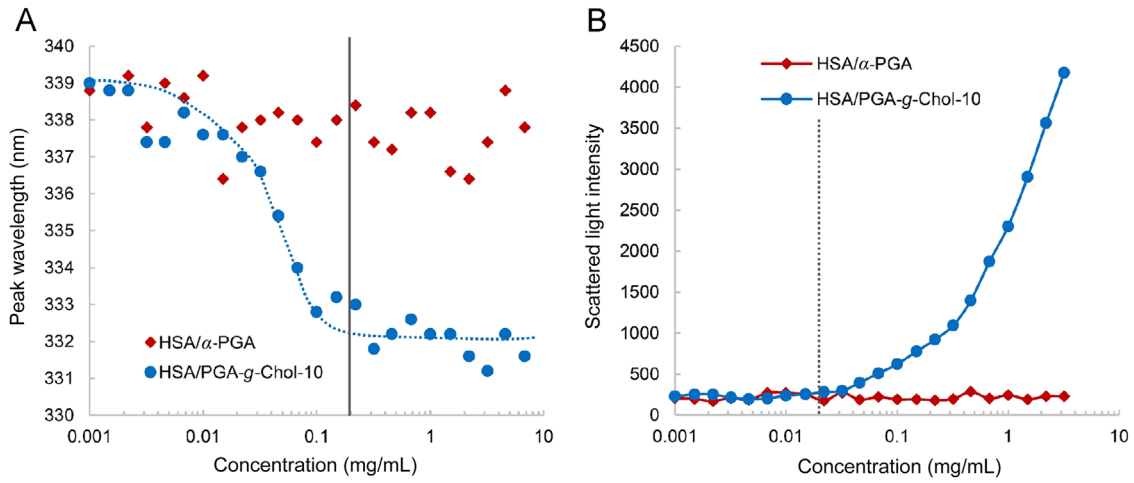

Figure 4 (A) Fluorescence emission peak wavelength of HSA plotted versus α-PGA and PGA-*g*-Chol-10 concentrations. The vertical full line represents that the PGA-*g*-Chol-10 concentration equals to that of HSA (5 μmol/L). The excitation wavelength was set at 295 nm. (B) Scattered light intensity (593 nm) of HSA/α-PGA and HSA/PGA-*g*-Chol-10 systems obtained from fluorescence measurements plotted versus α-PGA and PGA-*g*-Chol-10 concentrations. The vertical dashed line represents CAC of PGA-*g*-Chol-10 as determined by the pyrene fluorescence method.

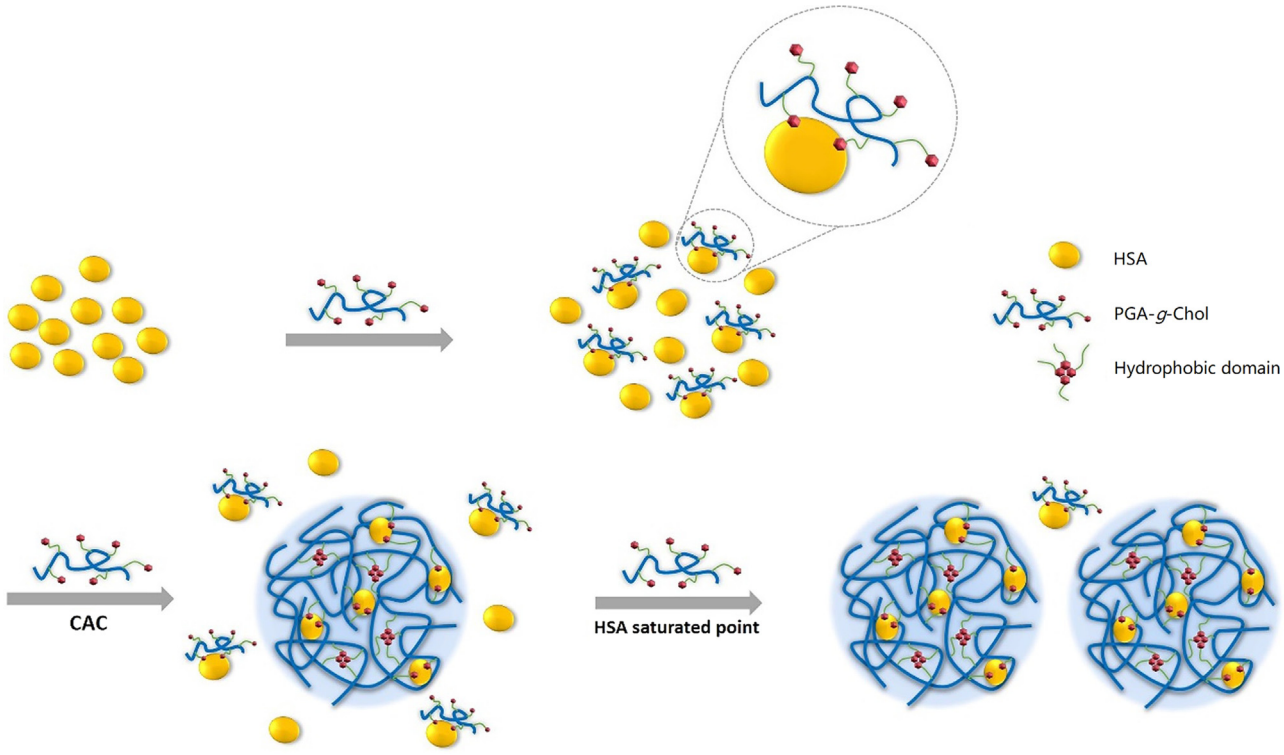

Figure 5 The proposed physical picture of HSA/PGA-*g*-Chol system.

PGA polymers, but there were perturbations of the secondary structure and the effect of PGA-*g*-Chol is obviously larger than that of α-PGA (Fig. 3). This suggests that both α-PGA and PGA-*g*-Chol can bind with HSA and the interaction between HSA and PGA-*g*-Chol is stronger.

Next, we characterized the protein/polymer system by measuring the protein self-fluorescence changes in the presence of polymers at different concentrations. The excitation wavelength was set at 295 nm, so the shift of the emission peak wavelength (around 330–340 nm) indicated the change of the microenvironment polarity of the sole tryptophan residue in HSA. Specifically, a blue shift means that the microenvironment around tryptophan becomes less polar[18,19]. Meanwhile, we used the 593 nm fluorescence signal, which is basically the scattered light intensity at 90°, to monitor the aggregate formation. As shown in Fig. 4, over the tested polymer concentration range (up to 10 mg/mL), the presence of α-PGA in the HSA solution caused little change of the microenvironment of its tryptophan residue, and apparently little aggregate formed in the solution at the same time. These results suggest that α-PGA, as a negatively-charged polypeptide, did not aggregate either by itself or with HSA. In

dramatic contrast, as the PGA-*g*-Chol concentration increases from 0 to 0.2 mg/mL, the peak wavelength of HSA gradually shifts from 339 to 332 (Fig. 4A), which suggests that the microenvironment of tryptophan became less polar. Further increase in the polymer concentration beyond 0.2 mg/mL does not change the emission peak wavelength of HSA any more. In the meantime (Fig. 4B), when the polymer concentration reaches 0.02 mg/mL and higher, the scattered light intensity at 593 nm increases significantly, suggesting the formation of aggregates in the solution. The transition point in the polymer concentration (*i.e.*, 0.02 mg/mL, as indicated by the vertical dashed line in Fig. 4B) is consistent with the previously determined CAC of PGA-*g*-Chol-10.

It is more interesting to note that the PGA-*g*-Chol concentration at which the blue shift of the HSA emission peak was saturated (*i.e.*, 0.2 mg/mL as indicated by the vertical full line in Fig. 4A, details of the calculation can be found in the Supporting Information), approximately corresponded to the molar concentration of the protein (5 μmol/L). Considering that there are two binding sites for cholesterol on HSA[20] and each PGA-*g*-Chol-10 polymer chain contains 6–20 cholesterol units, a possible explanation is that HSA and PGA-*g*-Chol-10 bind with each other at 1:1 ratio. When the PGA-*g*-Chol concentration was lower than that of HSA, more and more HSA molecules were bound by PGA-*g*-Chol as more polymers were added in the solution, and the emission peak wavelength gradually shifted to lower wavelength. After the amount of PGA-*g*-Chol is close to that of HSA (5 μmol/L, that is 0.2 mg/mL for PGA-*g*-Chol), all HSA molecules were bound with the polymer, and the emission peak wavelength did not shift any more.

Based on these data, we propose the following picture for HSA interacting with PGA-*g*-Chol in aqueous solution. As schematically shown in Fig. 5, each protein has several binding sites for the cholesterol moieties. As PGA-*g*-Chol polymers were added to the protein solution, the protein and the polymer formed complexes with the average ratio close to 1:1. The polymer binding changed the microenvironment around the tryptophan residue, and hence caused blue shift in its fluorescence emission peak (Fig. 4). When the concentration of polymer was equal to that of the protein (0.2 mg/mL or 5 μmol/L, as indicated by the vertical full line in Fig. 4A), all proteins were complexed, and the shift in tryptophan fluorescence emission peak leveled off. The 1:1 complexation between HSA and PGA-*g*-Chol seems reasonable for two reasons: (1) as previously described, each PGA-*g*-Chol chains has 6–20 cholesterol residues, which are enough to saturate the two binding sites on one protein. In addition, due to the multivalent binding effect[21], the scenario that all the binding sites of one protein are bound by one polymer chains is preferred than the other scenario where the binding sites were shared by multiple polymers (*i.e.*, the latter suffers more in term of polymer translational entropy penalty); (2) After one PGA-*g*-Chol bound to the protein *via* hydrophobic interactions, the un-conjugated fractions of the negatively-charged polyglutamate chain would form a corona around the protein, which in turn would prevent the binding of another polymer chains of the same charge.

In the meantime, the HSA/PGA-*g*-Chol complexation still left most of the hydrophobic cholesterol residues in the polymer chain un-bound. As the polymer concentration reached around the CAC of PGA-*g*-Chol (0.02 mg/mL, as indicated by the vertical dashed line in Fig. 4B), the polymers started to form aggregate of ~200 nm in diameter *via* hydrophobic association. More importantly, the HSA/PGA-*g*-Chol complex also participated in this aggregation *via* the same cholesterol residues which were not bound to the protein (Fig. 5). Through this interplay between polymer-protein binding and the polymer self-aggregation, both *via* the cholesterol units, the proteins were spontaneously encapsulated into the nanoparticles. In contrast, the un-modified polyglutamate polymers do not self-aggregate, and therefore, even though they may bind with the protein, no encapsulation would occur.

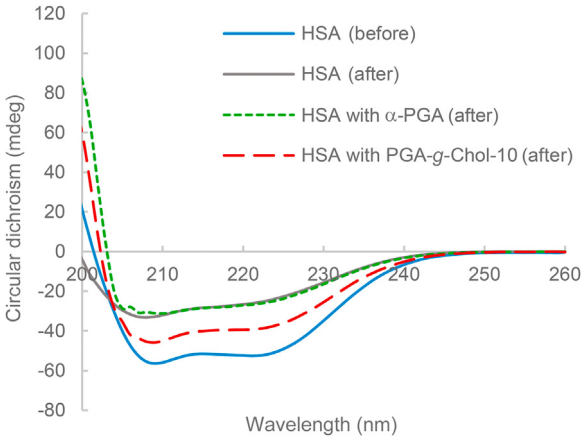

Figure 6 CD spectra of HSA (5 μmol/L) before and after thermal treatment at 90 °C for 1 h. The concentrations of α-PGA and PGA-*g*-Chol-10 were both 1.0 mg/mL. The spectrum of HSA with PGA-*g*-Chol-10 (or α-PGA) was obtained by subtracting PGA-*g*-Chol (or α-PGA) spectrum (also after the same thermal treatment) from those of the HSA/PGA-*g*-Chol (or α-PGA) mixture solutions.

3.4. *Thermal stability of the encapsulated HSA*

To further characterize the HSA/polymer system, we tested the thermal stability of HSA with and without the presence of α-PGA and PGA-*g*-Chol. As shown by the CD spectra in Fig. 6, after incubated at 90 °C for 1 h, there were significant changes in the HSA secondary structure. The presence of α-PGA in the solution at 1.0 mg/mL showed little mitigation on the structure change. In contrast, PGA-*g*-Chol at 1.0 mg/mL, which was higher than both its CAC and the protein concentration, demonstrated significant mitigation effect on the thermal denaturation. The encapsulation of proteins in the nano-aggregates improved their thermal stability, which is consistent with previous studies[10,11].

4. Conclusions

Hydrophobically modified polypeptides have the potential to become a platform material for the sustained release of protein drugs. In this study, we used cholesterol-grafted polyglutamate (PGA-*g*-Chol) and human serum albumin (HSA) as the model polymer and protein, respectively, and characterized their interactions in detail through fluorescence, circular dichroism, and light scattering. From these characterizations, a possible physical picture of the protein/polymer system emerged. In this proposed picture, the PGA-*g*-Chol polymer forms 1:1 complex with HSA through its pendant cholesterol residues and the corresponding two cholesterol-binding sites on the protein. In the protein/polymer complex, there are excess, unbound cholesterol residues along the polymer chain. As the polymer concentration increased beyond its critical aggregation concentration, the polymers self-associate *via* the excess cholesterol residues and form aggregates of ~200 nm

in diameter. Importantly, both the un-complexed and protein-complexed PGA-*g*-Chol participate this aggregation, and consequently the protein is encapsulated into the nanoparticles in its polymer-complexed form. This proposed physical picture clarifies our understanding and can be used to guide further development of this platform technology[22–25].

Acknowledgments

This work was supported by the National Natural Science Foundation of China (Grant No. 21434008).

Appendix A. Supporting information

Supplementary data associated with this article can be found in the online version at https://doi.org/10.1016/j.apsb.2018.08.001.

References

1 Leader B, Baca QJ, Golan DE. Protein therapeutics: a summary and pharmacological classification. *Nat Rev Drug Discov* 2008;**7**:21–39.
2 Mitragotri S, Burke PA, Langer R. Overcoming the challenges in administering biopharmaceuticals: formulation and delivery strategies. *Nat Rev Drug Discov* 2014;**13**:655–72.
3 Choi HS, Liu W, Misra P, Tanaka E, Zimmer JP, Ipe BI, et al. Renal clearance of quantum dots. *Nat Biotechnol* 2007;**25**:1165–70.
4 Pakulska MM, Miersch S, Shoichet MS. Designer protein delivery: from natural to engineered affinity-controlled release systems. *Science* 2016;**351**:aac4750.
5 Wills RJ, Dennis S, Spiegel HE, Gibson DM, Nadler PI. Interferon kinetics and adverse reactions after intravenous, intramuscular, and subcutaneous injection. *Clin Pharmacol Ther* 1984;**35**:722–7.
6 Tracy MA. Development and scale-up of a microsphere protein delivery system. *Biotechnol Prog* 1998;**14**:108–15.
7 Vermonden T, Censi R, Hennink WE. Hydrogels for protein delivery. *Chem Rev* 2012;**112**:2853–88.
8 Chan YP, Meyrueix R, Kravtzoff R, Nicolas F, Lundstrom K. Review on Medusa®: a polymer-based sustained release technology for protein and peptide drugs. *Expert Opin Drug Deliv* 2007;**4**:441–51.
9 Ibrahim A, Meyrueix R, Pouliquen G, Chan YP, Cottet H. Size and charge characterization of polymeric drug delivery systems by Taylor dispersion analysis and capillary electrophoresis. *Anal Bioanal Chem* 2013;**405**:5369–79.
10 Akiyoshi K, Deguchi S, Moriguchi N, Yamaguchi S, Sunamoto J. Self-aggregates of hydrophobized polysaccharides in water-formation and characteristics of nanoparticles. *Macromolecules* 1993;**26**:3062–8.
11 Sasaki Y, Akiyoshi K. Nanogel engineering for new nanobiomaterials: from chaperoning engineering to biomedical applications. *Chem Rec* 2010;**10**:366–76.
12 Lee EH, Kamigaito Y, Tsujimoto T, Uyama H, Sung MH. Synthesis of an amphiphilic poly(gamma-glutamic acid)-cholesterol conjugate and its application as an artificial chaperone. *J Microbiol Biotechnol* 2010;**20**:1424–9.
13 Ma Q, Li B, Yu YY, Zhang Y, Wu Y, Ren W, et al. Development of a novel biocompatible poly(ethylene glycol)-block-poly(γ-cholesterol-L-glutamate) as hydrophobic drug carrier. *Int J Pharm* 2013;**445**:88–92.
14 Lai JJ, Huang YB. Fibril aggregates of the poly(glutamic acid)–drug conjugate. *RSC Adv* 2015;**5**:48856–60.
15 Proksch GJ, Bonderman DP. Water-soluble cholesterol derivative for use in augmenting serum control materials. *Clin Chem* 1978;**24**:1924–6.
16 Pineiro L, Novo M, Al-Soufi W. Fluorescence emission of pyrene in surfactant solutions. *Adv Colloid Interface Sci* 2015;**215**:1–12.
17 Schartl W. *Light scattering from polymer solutions and nanoparticle dispersions*. Berlin: Springer-Verlag; 2007.
18 Lakowicz JR. In: *Principles of Fluorescence Spectroscopy*. 3rd ed. Berlin: Springer-Verlag; 2006.
19 Lai JJ, Yan HY, Liu Y, Huang YB. Effects of PEG molecular weight on its interaction with albumin. *Chin J Polym Sci* 2015;**33**:1373–9.
20 Ha JS, Ha CE, Chao JT, Petersen CE, Theriault A, Bhagavan NV. Human serum albumin and its structural variants mediate cholesterol efflux from cultured endothelial cells. *Biochim Biophys Acta* 2003;**1640**:119–28.
21 Fasting C, Schalley CA, Weber M, Seitz O, Hecht S, Koksch B, et al. Multivalency as a chemical organization and action principle. *Angew Chem* 2012;**51**:10472–98.
22 Lin TT, Liu EG, He HN, Shin MC, Moon C, Yang VC, et al. Nose-to-brain delivery of macromolecules mediated by cell-penetrating peptides. *Acta Pharm Sin B* 2016;**6**:352–8.
23 Ha D, Yang NN, Nadithe V. Exosomes as therapeutic drug carriers and delivery vehicles across biological membranes: current perspectives and future challenges. *Acta Pharm Sin B* 2016;**6**:287–96.
24 Wagner AM, Gran MP, Peppas NA. Designing the new generation of intelligent biocompatible carriers for protein and peptide delivery. *Acta Pharm Sin B* 2018;**8**:147–64.
25 Zhang YJ, Sun T, Jiang C. Biomacromolecules as carriers in drug delivery and tissue engineering. *Acta Pharm Sin B* 2018;**8**:34–50.